

Single B Production through R-Parity Violation

Ben O'Leary *

*SUPA, School of Physics, University of Edinburgh,
Edinburgh EH9 3JZ, Scotland, U.K.*

December 2, 2024

Abstract

Supersymmetry without R -parity predicts tree level quark flavor violation. We present a potential signal of single bottom production at electron-positron colliders with energies in the range 6 to 20 GeV. Taking into account rare decay limits it should be detectable with the current BaBar and Belle data samples.

1 Introduction

The Minimal Supersymmetric Standard Model [1] (MSSM) without R -parity [2] predicts Yukawa interactions that violate baryon and/or lepton number without violating Standard Model gauge symmetries or supersymmetry. The superpotential for these interactions is

$$W_{\mathcal{R}} = \frac{1}{2}\lambda_{ijk}(L_i)_a\epsilon_{ab}(L_j)_bE_k^c + \lambda'_{ijk}(L_i)_a\epsilon_{ab}(Q_j)_bD_k^c + \mu'_i(L_i)_a\epsilon_{ab}(H_u)_b + \frac{1}{2}\lambda''_{ijk}U_i^cD_j^cD_k^c \quad (1)$$

where i, j and k are generational indices and a and b are $SU(2)$ indices. Color indices have been suppressed. L is the lepton doublet, E^c is the charged anti-lepton singlet, Q is the quark doublet, D^c is the down-type anti-quark singlet, U^c is the up-type anti-quark singlet and H_u is the Higgs doublet which generates mass for up-type quarks. The factor of $1/2$ before the λ term is conventional: we see that $\lambda_{ijk} = -\lambda_{jik}$ by relabelling a to b and vice-versa in the first term of the superpotential, hence the extra factor of $1/2$ sets the coupling of the $\nu_i e_j E_k^c$ term to be λ_{ijk} rather than $2\lambda_{ijk}$. Likewise λ''_{ijk} is antisymmetric in j and k (the color indices in the final term are combined with an antisymmetric tensor), hence its factor of $1/2$.

The combination of λ' and λ'' leads to proton decay and is thus constrained by proton disappearance searches [3] and searches for proton decay into a positron and a pion [4]. Requiring $\lambda''_{ijk} = 0$ is sufficient to guarantee perturbative proton stability while leaving the possibility of non-zero lepton-number violating couplings. These couplings introduce a new channel for flavor violation.

*ben.oleary@ed.ac.uk

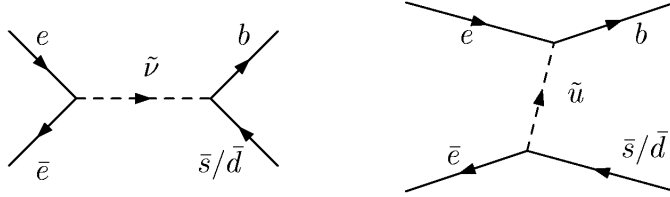


Figure 1: Sneutrino- and squark-mediated single b production diagrams.

So far, there is no direct evidence for supersymmetry or R -parity violation. The non-observation of single sparticle production puts constraints on a combination of their masses and couplings [5]. Most of the tightest bounds on individual couplings come from charged current universality [6], as single sfermion exchange generally interferes with weak boson exchange. Meson and τ -lepton rare decay data typically provide tighter bounds on products of RPV couplings than the product of individual bounds [2].

In an era of high-precision flavor physics the obvious question is whether for example B physics observables can be used to further probe the RPV parameter space. We present a potential signal of single B production at electron-positron colliders with energies in the range 6 to 20 GeV, with special attention given to the case of a center-of-mass energy of 10.58 GeV, at which BaBar and Belle currently run. The lower limit is chosen slightly above the threshold for creating a BK meson pair.

2 Single b Production

The Standard Model predicts quark flavor violation through CKM mixing, but the cross-sections for $e\bar{e}\rightarrow b\bar{s}$ or $b\bar{d}$ are extremely small. Detection of flavor violation in significant excess to the Standard Model prediction would be an exciting signal of new physics.

In the MSSM without R -parity, flavor violation can be mediated at tree level by sfermions. A non-zero λ and λ' combination allows single b quark production along with a light down-type anti-quark through the Feynman diagrams shown in figure 1.

The sneutrino mediated diagram is proportional to λ_{g11}^* ($e\bar{e}\tilde{\nu}$ vertex) multiplied by either λ'_{g23} ($\tilde{\nu}b\bar{s}$ vertex) or λ'_{g13} ($\tilde{\nu}b\bar{d}$ vertex). The squark mediated diagram is proportional to λ'_{1g3} ($eb\tilde{u}$ vertex) multiplied by either λ_{1g2}^* ($\tilde{u}\bar{e}\bar{s}$ vertex) or λ_{1g3}^* ($\tilde{u}\bar{e}\bar{d}$ vertex). We write $\tilde{\nu}$ and \tilde{u} instead of $\tilde{\nu}_L^g$ and \tilde{u}_L^g to avoid clutter — in all cases the sfermion is implicitly of generation g , and associated with the left-handed chirality of its superfield partner.

Because the sfermions are constrained to be heavy, $m_{\tilde{\nu},\tilde{u}}\gtrsim 100$ GeV $\gg \sqrt{s}$, we approximate their propagators as static $1/m_f^2$. Moreover, we assume that one sfermion dominates the signal process, either because it is lighter than the others or because it has a larger coupling product.

If we sum over the b and \bar{b} final states and allow for only one of the two R -

coupling	bound	process
$ \lambda_{g11} ^2 \lambda'_{g13} ^2 m_{\tilde{\nu}}^{-4}$	$2.9 \times 10^{-18} \text{ GeV}^{-4}$	$B_d^0 \rightarrow e\bar{e}$ [2]
$ \lambda_{g11} ^2 \lambda'_{g23} ^2 m_{\tilde{\nu}}^{-4}$	$2.0 \times 10^{-16} \text{ GeV}^{-4}$	$B_s^0 \rightarrow e\bar{e}$ [2]
$ \lambda'_{1g1} ^2 \lambda'_{1g3} ^2 m_{\tilde{u}}^{-4}$	$2.9 \times 10^{-13} \text{ GeV}^{-4}$	APV in Cs [8], A_{FB}^b [2]
$ \lambda'_{1g2} ^2 \lambda'_{1g3} ^2 m_{\tilde{u}}^{-4}$	$7.4 \times 10^{-17} \text{ GeV}^{-4}$	$B_s^0 \rightarrow K e\bar{e}$ [9]

Table 1: Bounds on coupling combinations. The atomic parity violation bound on $|\lambda'_{1g1}|^2 m_{\tilde{u}}^{-2}$ is combined with the constraint on $|\lambda'_{1g3}|^2 m_{\tilde{u}}^{-2}$ from the bottom forward-backward asymmetry.

bd via $\tilde{\nu}$	$1.4 \times 10^{-5} \text{ fb}$	$bd\gamma$ via $\tilde{\nu}$	$1.6 \times 10^{-9} \text{ fb}$
bs via $\tilde{\nu}$	$9.7 \times 10^{-4} \text{ fb}$	$bs\gamma$ via $\tilde{\nu}$	$1.1 \times 10^{-7} \text{ fb}$
bd via \tilde{u}	0.54 fb	$bd\gamma$ via \tilde{u}	$6.0 \times 10^{-5} \text{ fb}$
bs via \tilde{u}	$1.4 \times 10^{-4} \text{ fb}$	$bs\gamma$ via \tilde{u}	$1.5 \times 10^{-8} \text{ fb}$

Table 2: The cross-sections for $e\bar{e} \rightarrow b\bar{s}/s\bar{b}/b\bar{d}/d\bar{b}/b\bar{s}\gamma/s\bar{b}\gamma/b\bar{d}\gamma/d\bar{b}\gamma$ at $\sqrt{s} = 10.58 \text{ GeV}$.

parity violating processes to dominate we obtain the differential cross-sections

$$\frac{d\sigma}{d\Omega} = \frac{|\mathbf{p}_b|}{|\mathbf{p}_e|} \frac{3}{128\pi^2} (s - m_b^2 - m_s^2) \frac{|\lambda_{g11}|^2 |\lambda'_{g23}|^2}{m_{\tilde{\nu}}^4} \quad (2)$$

for the s -channel sneutrino exchange, and

$$\frac{d\sigma}{d\Omega} = \frac{|\mathbf{p}_b|}{|\mathbf{p}_e|} \frac{3}{128\pi^2 s} (t - m_b^2) (t - m_s^2) \frac{|\lambda'_{1g2}|^2 |\lambda'_{1g3}|^2}{m_{\tilde{u}}^4} \quad (3)$$

for the t -channel squark. \mathbf{p}_b is the 3-momentum of the b quark. We have ignored the electron mass compared to the rest of the masses and energies. The case of a final-state down quark can be obtained by the appropriate changes of indices. The current limits on these combinations of couplings from experimental data¹ are given in table 1.

In calculating the signal, we assume that the values of the couplings are equal to their current bounds. Performing the angular integrations (restricted to $|\cos(\theta)| \leq 0.9$) leads to the cross-sections presented in figure 5 and figure 6, with the numerical values for $\sqrt{s} = 10.58 \text{ GeV}$ given in table 2.

2.1 Single b Production With A High-Energy Photon

As is discussed in section 3, the production of a single B meson — light meson pair is not necessarily a clean signal. B mesons are often misidentified, and an accurate reconstruction of the kinematics may reduce the detection efficiency substantially. Here we consider the cases of an additional final-state photon for the signals considered above, which may prove to be a cleaner signal as

¹We do not agree with the bounds from sneutrino-mediated B -decay given in [2], as we disagree with the formula presented in [7], equation (13), which [2] uses with updated data. However, we only disagree by a factor of 4, which is not enough to raise the signal beyond the attobarn level.

the energy of the B meson does not have to be measured — for a sufficiently energetic photon, $B\bar{B}$ pair production is kinematically excluded (in analogy to using radiative return to measure hadronic cross-sections for lower energies than those at which an experiment runs [10]). The Feynman diagrams are the same as in figure 1, but with an external photon emitted by any of the external particles. An emission by the virtual squark suppresses the matrix element by another power of $m_{\tilde{u}}^2$. We make a restriction on the photon to exclude the possibility that it was emitted through the radiative decay of a B meson. Since there is an upper bound to the energy that the radiated photon can have for a B meson with a given momentum in the beam center-of-momentum frame, we restrict the photon to have 10% or more energy above this value for a B meson with half the beam energy, *i.e.*

$$E_\gamma \geq 1.1 \frac{m_B^2}{2((\sqrt{s}/2) - \sqrt{s/4 - m_B^2})} \quad (4)$$

In doing this, we eliminate the background of misidentified $B\bar{B}$ pair production.

The cross-sections for this process are also presented in figure 5 and figure 6, with the numerical values for $\sqrt{s} = 10.58$ GeV given in table 2. The signal begins at 10.56 GeV as below this it is kinematically impossible to produce a $B\bar{B}$ pair, hence the advantage of the additional photon is non-existent, while still suffering from the α suppression of the signal. The restriction on the photon energy cuts out much of the phase space, and cuts out more as \sqrt{s} increases, until around $\sqrt{s} = 13.8$ GeV, where the entire phase space is excluded. Unfortunately, even in the best case, close to the special value $\sqrt{s} = 10.58$ GeV, the best signal is less than 0.1 ab.

2.2 Experimental Signature

The signal calculated above has on-shell single quarks in the final state. The process of hadronization is not well understood, but since $\sqrt{s} \gg \Lambda_{\text{QCD}}$ we assume that the scattering amplitude for the sum of all possible $e\bar{e} \rightarrow M\bar{B}$ is the same as for $e\bar{e} \rightarrow b\bar{q}$, where M is a light (bottomless) meson which has anti-quark constituent \bar{q} . In this scheme, the production of a $b\bar{d}$ pair leads to an on-shell neutral pair with an unflavored light meson ($\bar{B}_d\pi^0$, $\bar{B}_d\eta'$, $\bar{B}_d\eta'$, $\bar{B}_d^*\rho$ or $\bar{B}_d^*\omega$) 43.5% of the time and to a charged pair with an unflavored light meson ($B_d^-\pi^+$, $B_d^-\rho^+$) 43.5% of the time, according to the Lund string model [11]. The remaining 13% consist of the channels where the light meson is strange ($\bar{B}_s K$ and $\bar{B}_s^* K^*$).

3 Background

We identify three sources of background to the signal: direct SM $e\bar{e} \rightarrow M\bar{B}$, misidentified $B\bar{B}$ pair production, and R -parity conserving MSSM $e\bar{e} \rightarrow b\bar{s}$ or $b\bar{d}$.

3.1 Standard Model Background

As mentioned in the introduction, there is a Standard Model background to the processes $e\bar{e} \rightarrow b\bar{s}$, $b\bar{d}$. However, its leading order contribution is at one-loop level

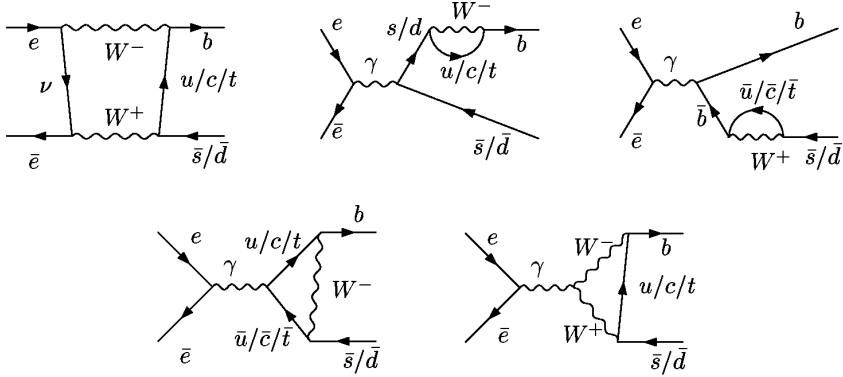


Figure 2: SM background single b production.

bd in SM	7.3×10^{-6} fb
bs in SM	1.8×10^{-4} fb

Table 3: SM background cross-sections for $e\bar{e} \rightarrow b\bar{s}/s\bar{b}/b\bar{d}/d\bar{b}$ at $\sqrt{s} = 10.58$ GeV.

and doubly Cabibbo suppressed. Ignoring Feynman diagrams with a electron-Higgs Yukawa coupling, there are five classes of diagrams, shown in figure 2.

Using FeynArts [12] and FormCalc [13], which utilize FORM [14] and LoopTools [13], we obtain the cross-sections presented in figure 5 and figure 6, with the numerical values for $\sqrt{s} = 10.58$ GeV given in table 3.

Considering the two-particle final states, the SM background is completely negligible compared to the squark-mediated signal for bd production. However, it is within an order of magnitude of the other three potential signals. Unfortunately, detecting such cross-sections of 10^{-4} fb is well beyond the reach of current colliders.

There are related processes, where four quarks are created in the hard process. They can then hadronize into two mesons, either a charged pair or a neutral pair. The diagrams for the production of a charged pair are those in figure 3. Those for the production of a neutral pair are the same as for the charged pair, but with the down-type quarks combining to form a \bar{B}^0 and the up-types combining to form a light neutral meson.

Generally, we expect the hard matrix element for the creation of four quarks to be of a similar size or less than the two-quark case. Even ignoring the suppression of the wavefunction overlap of these four quarks with the two-meson final state, we can therefore safely neglect this Standard Model background as well.

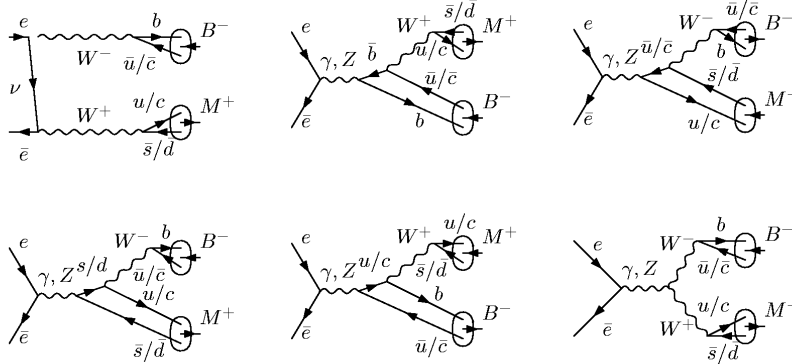


Figure 3: Four-quark SM single B meson production.

3.2 False Signal From $B\bar{B}$ Pair Production

Misidentification of B mesons is an extremely important concern. Our signal must not be confused with that of a $b\bar{b}$ pair production with one unidentified b . Simply looking for events that contain only a single tagged bottom is (quantitatively) not feasible. Hence, we use kinematics to get rid of $b\bar{b}$ events. The direct production of a B meson and a light meson of mass m_M leads to, in the beam center-of-mass frame, the B meson taking a fraction $(s + m_B^2 - m_M^2)/(2s)$ of the center-of-mass energy \sqrt{s} . For the squark-mediated bd signal with $\sqrt{s} = 10.58$ GeV, the B meson will have energy between 6.56 GeV (where the light meson is an η') to 6.61 GeV (where the light meson is a π^0). This is to be compared to the case of $B\bar{B}$ production, where both have energy 5.29 GeV.

The high-energy tail of the electron-positron beam can create $b\bar{b}$ pairs with enough energy that the resulting B mesons could present a false signal by both having the energy that a singly-produced B meson would have (around 6.6 GeV for $\sqrt{s} = 10.58$ GeV), and one could decay into a high-energy light meson, with the radiated photon or particle missing the detector. BaBar produces 1.1×10^6 $b\bar{b}$ pairs per fb^{-1} , and has over 350 fb^{-1} of integrated luminosity recorded [15]. This gives 385 million $b\bar{b}$ pairs. The beam energy spread we expect to be of the order of 5 MeV, estimated from the beam spread from 4.63 to 4.83 MeV on the $\Upsilon(4S)$ resonance [16]. For the false signal described, the $B\bar{B}$ -pair is required to have 2.6 GeV more than the mean beam energy. This is over 400 standard deviations away, if we assume that the beam energy has a Gaussian distribution. The expected number of events from this channel is then insignificant (less than 10^{-250}).

Using the $\Upsilon(4S)$ resonance width of 20.7 MeV [16] as the spread, the cut is 125 standard deviations away from the mean, which still leads to an expected number of events less than 10^{-250} . These brief estimates certainly allow us to neglect beam energy spread as a background source for our signal process.

This is also the source of any potential background to the case with an additional high-energy photon. For the range of energies considered, the false

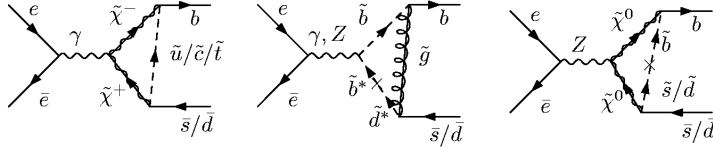


Figure 4: Example MSSM background diagrams: (a): flavor violation through $SU(2)_L$; (b, c): flavor violation through a mass insertion on the squark line. (b) is known as a *pengluino* diagram.

signal background of a $B\bar{B}$ plus a high-energy photon requires between 1 and 2 GeV more than the mean beam energy. This is 200 to 400 standard deviations over the mean, and hence the expected number of events is less than 10^{-250} . The false signal background of a $B\bar{B}$ pair of sufficient energy that the radiative decay of one of the mesons produces a photon that passes the cut is also less than 10^{-250} events.

3.3 R-Parity Conserving MSSM Background

Any signal of flavor violation in significant excess of the SM prediction is an exciting signal for new physics. However, the thrust of this paper is that such a signal could come from RPV couplings. Backgrounds from the R -parity conserving part of the MSSM arise from two sources: flavor violation through $SU(2)_L$ and through non-minimal squark mixing, *i.e.* general soft SUSY breaking terms [17]. (Examples of both types are shown in figure 4.)

The diagrams for the former case are easily obtained by replacing the Standard Model particles in SM background loops with their supersymmetric partners. The W boson mass ($m_W \gg m_B$) accounts for most of the suppression of the SM background. The sparticle masses are constrained to be (considerably) larger than m_W . The structure of the amplitude is similar, which means that we can expect the SUSY loops without a new flavor structure to contribute below the level of the SM backgrounds. If we increase the largest sparticle mass in the loop to three times the W boson mass, these SUSY backgrounds drop below 10% to the already negligible Standard Model background rate. There are potential enhancements in the large $\tan(\beta)$ region of the MSSM parameter space, but in the Higgs sector these destructively interfere with the SM amplitude [18], while any other enhancements are constrained by $b \rightarrow d\gamma$ to be at most close to the SM value.

The diagrams describing contributions from non-minimal flavor structure in squark sector are obtained by “supersymmetrizing” the virtual particles in the loops in the one-loop corrections to $e\bar{e} \rightarrow b\bar{b}$ (except for those diagrams without a virtual quark), and replacing the external \bar{b} with a \bar{d} and the internal \tilde{b} with the mass eigenstate mixtures of \tilde{b} and \tilde{d} . These contributions are not easy to calculate, as the most significant pengluino diagram (shown in figure 4), is proportional to $\alpha\alpha_s\delta m_q^2/m_q^2$, where δm_q^2 is the difference in the squared masses of the squarks². This, at least for b - d mixing, is not well constrained [19].

²This assumes that the gluino is more massive than the squarks, otherwise replace the

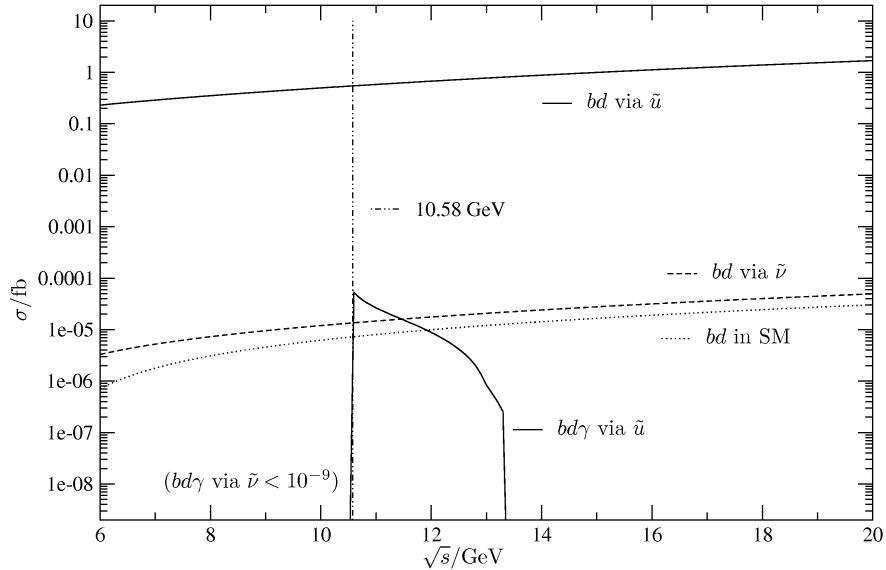


Figure 5: Cross-sections for $e\bar{e} \rightarrow b\bar{d}/d\bar{b}/b\bar{d}\gamma/d\bar{b}\gamma$ through R -parity violation and the SM background for $e\bar{e} \rightarrow b\bar{d}/d\bar{b}$.

However, we note that these diagrams would also contribute to $B \rightarrow \rho\gamma$, which is tightly constrained.

Altogether, we expect the R -parity conserving part of the RPV MSSM to contribute to the background at a rate comparable to the Standard Model contribution at most.

4 Outlook

As far as we are aware, there have been no searches for single B production. Currently BaBar has almost 400 fb^{-1} of integrated luminosity [15] and Belle has almost 650 fb^{-1} of data [20] available for analyses. Ignoring detector effects the maximum signal rate for single b production allowed by current bounds comes from t -channel squark exchange and could be as large as 500 events.

We have shown that the backgrounds to this process are negligible, which makes single b production a promising search channel for R parity violation.

5 Acknowledgements

I am grateful to Tilman Plehn, Michael Krämer, Thomas Binoth and Steve Playfer for useful discussions, and to Ulrich Nierste for reading the draft. B.O'L. is supported by the Carnegie Trust for the Universities of Scotland.

gluino mass with the mass of the more massive squark.

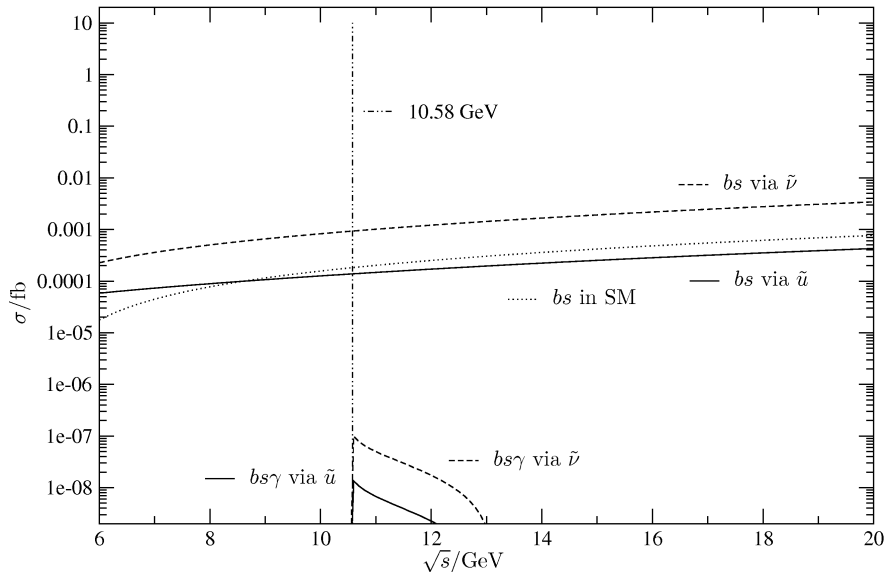


Figure 6: Cross-sections for $e\bar{e} \rightarrow b\bar{s}/s\bar{b}/b\bar{s}\gamma/s\bar{b}\gamma$ through R -parity violation and the SM background for $e\bar{e} \rightarrow b\bar{s}/s\bar{b}$.

References

- [1] for an introduction see *e.g.*: S. P. Martin, arXiv:hep-ph/9709356; I. J. R. Aitchison, arXiv:hep-ph/0505105.
- [2] R. Barbier *et al.*, Phys. Rept. **420** (2005) 1 [arXiv:hep-ph/0406039].
- [3] S. N. Ahmed *et al.* [SNO Collaboration], Phys. Rev. Lett. **92** (2004) 102004 [arXiv:hep-ex/0310030].
- [4] M. Shiozawa *et al.* [Super-Kamiokande Collaboration], Phys. Rev. Lett. **81** (1998) 3319 [arXiv:hep-ex/9806014].
- [5] S. Eidelman *et al.*, Phys. Lett. B **592**, 1 (2004) and 2005 partial update for the 2006 edition available on the PDG WWW pages (URL: <http://pdg.lbl.gov/>)
- [6] see *e.g.*: H. K. Dreiner, G. Polesello and M. Thormeier, Phys. Rev. D **65** (2002) 115006 [arXiv:hep-ph/0112228].
- [7] J. P. Saha and A. Kundu, Phys. Rev. D **66** (2002) 054021 [arXiv:hep-ph/0205046].
- [8] J. L. Rosner, Phys. Rev. D **65** (2002) 073026 [arXiv:hep-ph/0109239].
- [9] S. Nandi and J. P. Saha, arXiv:hep-ph/0608341.
- [10] G. Rodrigo, H. Czyz and J. H. Kuhn, eConf **C0209101** (2002) WE06 [Nucl. Phys. Proc. Suppl. **123** (2003) 167] [arXiv:hep-ph/0210287].

- [11] B. Andersson, G. Gustafson, G. Ingelman and T. Sjostrand, Phys. Rept. **97** (1983) 31.
- [12] T. Hahn, Comput. Phys. Commun. **140** (2001) 418 [arXiv:hep-ph/0012260].
- [13] T. Hahn and M. Perez-Victoria, Comput. Phys. Commun. **118** (1999) 153 [arXiv:hep-ph/9807565].
- [14] J. Vermaseren [arXiv:math-ph/0010025].
- [15] <http://bbr-onlwww.slac.stanford.edu:8080/babarrc/perfdata.html>
- [16] B. Aubert *et al.* [BABAR Collaboration], Phys. Rev. D **72** (2005) 032005 [arXiv:hep-ex/0405025].
- [17] L. J. Hall, V. A. Kostelecky and S. Raby, Nucl. Phys. B **267** (1986) 415.
- [18] H. E. Logan and U. Nierste, Nucl. Phys. B **586** (2000) 39 [arXiv:hep-ph/0004139].
- [19] M. B. Causse and J. Orloff, Eur. Phys. J. C **23** (2002) 749 [arXiv:hep-ph/0012113].
- [20] http://belle.kek.jp/bdocs/lum_day.gif